ON THE POSSIBILITY OF DATING AND ISOTOPIC PATTERN DETERMINATION FOR SAMPLES FROM THE DANUBE DELTA REGION VIA GAMMA RAY SPECTROMETRY

Silvia ISE[1], Radu ȘEREMET[1], Iulian ANDREICOVICI[1], Iulian POJAR[2], Bogdan ALEXANDRESCU[2], Sorin UJENIUC[3], Rareș ȘUVĂILĂ[2]

[1]University of Bucharest, Faculty of Physics, 405 Atomistilor St., 077125, Măgurele, Ilfov, Romania
[2]National Institute of Marine Geology and Geo-Ecology (GeoEcoMar), 23-25 Dimitrie Onciul St., 024053, Bucharest, Romania
e-mail: rares.suvaila@geoecomar.ro
[3]Horia Hulubei National Institute for Physics and Nuclear Engineering, 30 Reactorului St., 077125, Magurele, Ilfov, Romania

DOI: 10.xxxx

Abstract. Several samples from the Danube Delta region are analysed by gamma ray spectrometry in an attempt to quantify timing and precision associated to isotopic pattern determination and dating of recent sediments in a laboratory under development. Various detectors, electronic configurations and shielding options were used to test the detection limits and system stability on samples which were prepared and encapsulated in several ways. The results evidence the capacity of dealing with some 300 samples per year and per detector of 30% relative eficiency for an overall 5 to 8% relative uncertainty associated to typical activities of environmental samples.

Key words: gamma ray, environmental spectrometry, uncertainty budget, detection limits, natural series, anthropogenic radionuclides, multiparameter optimisation

1. INTRODUCTION

Gamma ray spectrometry is the most powerful non-destructive testing method when it comes to environmental sample nuclide identification. The detection limits are orders of magnitude higher than those of ICP-MS for example, but sample preparation consists in a minimal procedure and sample integrity is preserved. Also, in terms of radioactivity, there is no real hazard associated to the procedure (as long as neutron activation is not involved), for the gamma de-excitation is following alpha or beta decays of very low levels from the natural series present in such samples. Our team had a prior attempts on clay samples, including activation analysis (Olăcel *et al.,* 2022). This time the study focuses on a new setup under testing, with elements from cores originating from the Danube Delta, but which are in much lower quantities, down to a few grams. This requires a study of the detection thresholds, as the latter determine the validity and significance of any quantitative determination, such as the specific activities (counts/second/mass unit) which are of crucial interest for our work. The goal of this work is to determine the minimal conditions which ensure good precision (less than 10% errors) determinations of specific activities that lead to dating and isotopic pattern analysis for cores originating from this area without having to perform the measurements in an underground laboratory. The reason for which we intend to set those parameters is the number of samples in such a project is very large, hundreds to thousands, and it is very laborious to carry out the research in an underground facility. Consequently, our laboratory under development has to be optimised in terms of detector characteristics, shielding (now only 5 cm of lead), electronics for detection, peripherals (such as oven and milling devices), and also software tools.

2. MATERIALS AND METHODS

2.1. Mapping

Single beam morphological mapping was performed in order to determine water depth by measuring the time elapsed from acoustic signal emission to its reception after reflection on the bottom of the channel. The single beam system is equipped with a single transceiver, which is responsible for both emission and reception of the signal. For this work, the bathymetric measurements have been carried out with the help of a modern equipment on a light research vessel; the whole research infrastructure belongs to the NIRD for Geology and Geoecology GeoEcoMar from Romania. Measurements were performed with a single beam system, CeeLine Echosounder produced by CeeHydroSystems, operating at a 200 kHz frequency (Fig. 1). Bathymetric profiles have been planned equidistantly at 50 cm, as shown in figure 2. The resolution is 1.0 cm and the accuracy is 0.01 m ± 0.1% of the depth.

Fig. 1. Sounder for the CeeLine HydroSystems single beam system

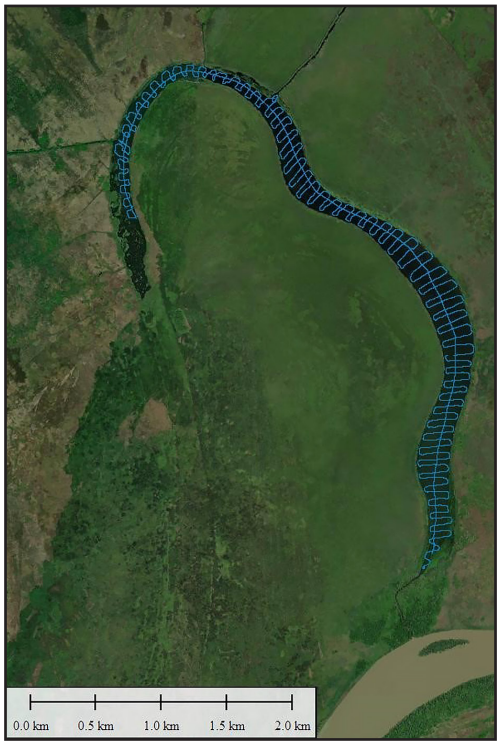

Fig. 2. Bathymetric profiles for Lake Erenciuc

The acquisition was carried out in the projection system UTM, Zone 35N, Datum WGS 84. Following the acquisition, raw data processing was carried out by filtering the errors with a specialised software, HydroMagic version 9. Figure 3 displays the bathymetric map of Lake Erenciuc. Its length is approximately 6.6 km and its width varies between 100 and 300 m, with depths between 0.9 and 3.2 m. The lower depths are localised at the entrance of the lake, on the side of the Erenciuc Channel, in the median zone (entrance of the Mocansca Channel which links it to the Puiu Lake) and towards the closing zone of the lake, where most of the surface is covered with vegetation. Those low depths are due to the sediment transport and deposition from the adjoining channels (Erenciuc and Mocansca).

2.2. SAMPLING AND SAMPLE PREPARATION

Three cores were taken from Lake Erenciuc, the spots coordinates being verified with good precision. Subsequently, the cores were sliced and all resulting samples were placed in the oven at 50°C until no mass change was noticed (this took approximately three days). Unfortunately, the resulting sample mass was very low, the order of 10 g per sample, which lead to poor statistics in the spectra. Also, each sample was corresponding to a 5 cm layer in average, which is too thick for precise dating.

Radioactive equilibrium between Rn descendants is always a challenge. Our approach was to seal the Petri boxes with silicone adhesive and check the weight constantly. Weighing the samples after silicone drying, before and after gamma measurement, showed a mass variation under 1%, between the three values.

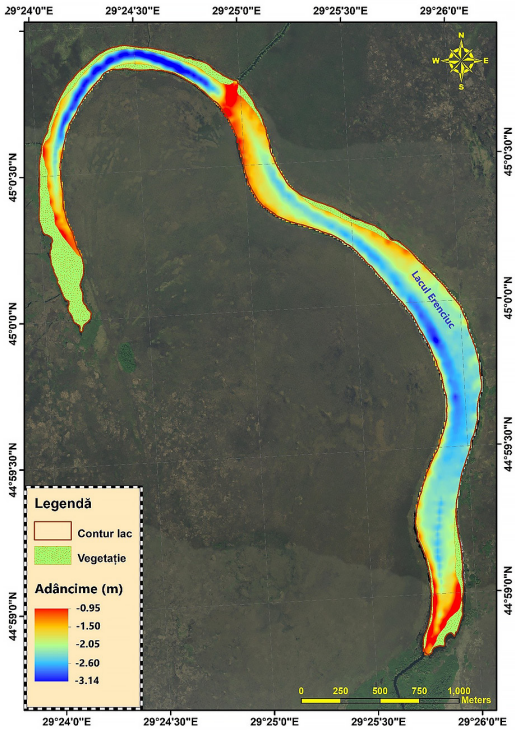

Fig. 3. Bathymetric map of Lake Erenciuc

This change in mass shows the water intake and consequently the possibility of air circulation (which means also Rn escape and radioactive equilibrium problems). However, given the balance precision of only two decimals and the small quantity of dry material available, we cannot draw a straight conclusion on the U-Ra chain equilibrium being kept based on this data. The reason for which sealing must be treated so carefully is that such procedures are not always successful and the equilibrium required for ^{226}Ra estimation via daughter products might not be reached. An important fact is the direct consequence of a ^{222}Rn loss is the systematic underestimation of the supported ^{210}Pb, which can affect ^{210}Pb dating and the resulting sedimentation rate estimation for sediment chronology.

In order to ensure sample uniformity, the dry material was milled as much as possible. Given the small size of sediment grains (under 100 μm) and the fact they were placed in the closest geometry possible to the detector end cap with an overall millimetric layer of autoabsorbtion (sample and Petri dish wall combined), uniformity was ensured at a satisfactory level.

2.3. Choice of detector and electronics

After testing various types of detectors in order to evaluate the strengths and weaknesses of a laboratory setup which is supposed to deal with a large number of samples in little time while keeping costs low and resolution high, the Hyper-Pure Germanium (HPGe) ones overcame all the other options, such as Ge(Li) - Germanium-Lithium - or Lanthanum/ Cerium Bromides, because of their energy resolution in first place. Although HPGe detectors are more expensive, their high efficiency recommends their use, as quantitatively spectra acquisition is equivalent to more than one detector of the other types, while the costs for shielding remain low, as we deal with a single one.

The detector used (Fig. 4) is a quite old but reliable n-type HPGe model MGX45P4-83, (ORTEC, 2007), with a relative efficiency of 47% at the energy of 1332 keV (60Co); the crystal dimensions are 61.5 mm in diameter, 73.4 mm length; rounded edges with a nominal radius of curvature of 8 mm; the inner hole measures 9.3 mm in diameter, its depth is of 65.1 mm and it ends with a spherical shape of 5 mm radius. The dead layer on the entrance face due to Boron implantation had a thickness of 0.3 microns; the inner contact is obtained by Li diffusion and had an initial thickness of 0.7 mm. It is quite possible those dimensions increased over time and supplementary Monte Carlo simulations have to be carried out in order to estimate them again. This is the only way to have a correct estimation, as a radioscopy would only evidence the shape of the crystal (Sima, 2022). The detector cup is made from 0.03 mm Al + 0.03 mm mylar on the entrance side, 0.8 mm Al on the sides and 3 mm Al on the back of the crystal. The entrance window is made from Be, with the thickness of 0.5 mm. The distance from the crystal to the entrance window is equal to 4 mm (Șuvăilă and Sima, 2011). Results from the Monte Carlo simulations of the source-detector ensemble in various geometries suggest the real distance is more likely close to 6 mm. The parameters of the detector, as specified in the manufacturer's sheets, are: Resolution (FWHM) at 1.33 MeV: 2.00 keV; Peak to Compton Ratio (60Co): 63:1; Peak Shape (FWTM / FWHM) at 1.33 MeV: 1.9; Peak Shape (FWFM/FWHM) at 1.33 MeV: 2.8; Resolution (FWHM) at 5.9 keV (55Fe) 640 eV.

The electronic modules we choose were produced by ORTEC, the most important being the amplifier model 671 and the multi-channel analyser (MCA) model 927 (Fig. 5). As a side note, the equivalent modules from CANBERRA exhibit the same performance level: the final choice was made as a function of availability and timing.

2.4. Setup testing, detection limits

While testing the setup, we proceeded to background or following the case blank spectrum analysis in order to evaluate the shielding and the Radon (Rn) purge effect by liquid nitrogen (LN_2): as ^{222}Rn is the heaviest noble gas originating from the natural Uranium-Radium series, we can find it anywhere, and its presence must be lowered, as we need to determine those elements' concentrations within the samples we analyse.

Fig. 4. HPGe detectors and related electronics; Petri dishes with sediment samples

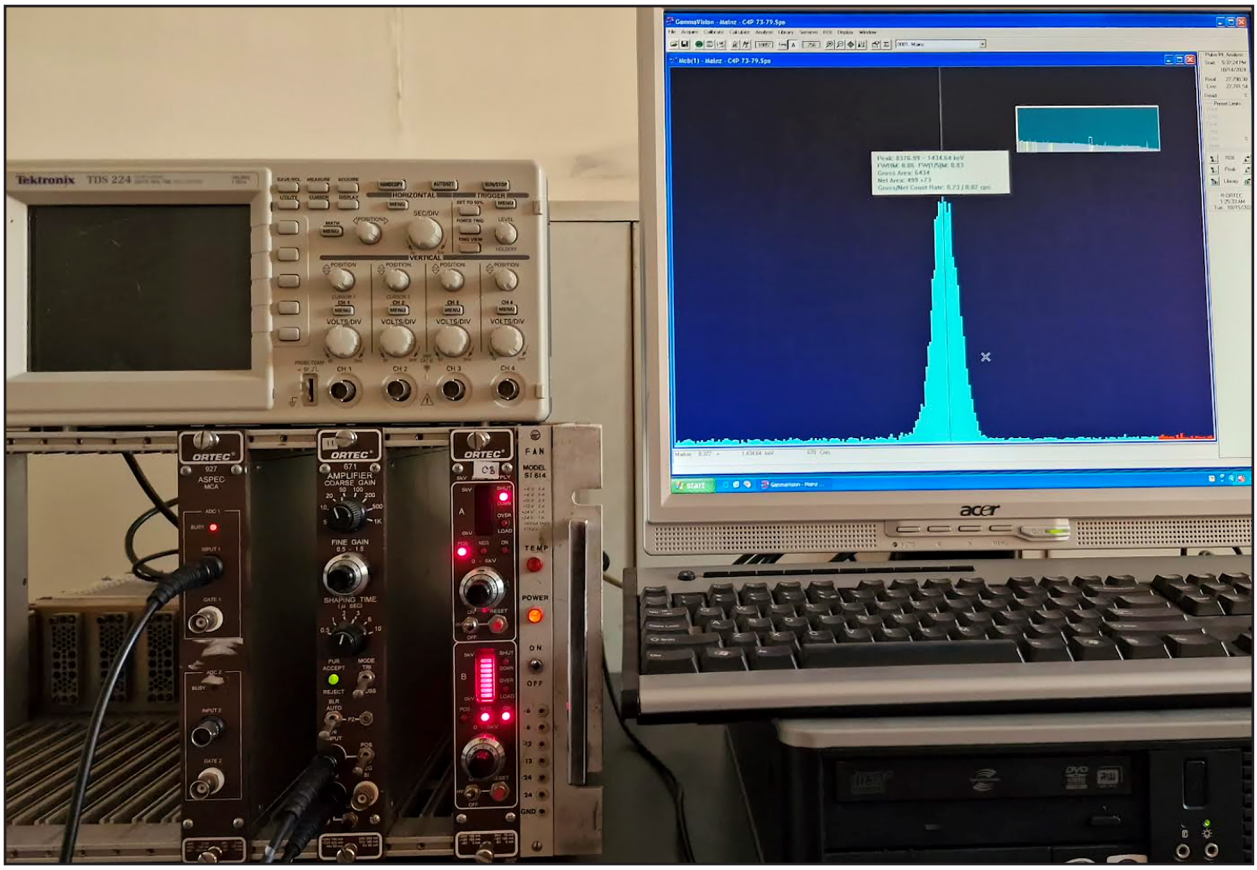

Fig. 5. Specific electronic modules used for the present work

Consequently, we proceeded to purging the vicinity of the detector with the evaporated LN_2 from the detector's Dewar vessel and lowered Rn activity by an order of magnitude.

Electronics were also tested for stability, not only performance, and the detection chain proved it keeps its parameters stable in time. Of course signal testing with an oscilloscope and blank spectra acquisition is a periodic necessity in order to guarantee those parameters remain stable.

As for the detection limits, in gamma spectrometry, three major limiting levels are used to make assumptions; those are the critical limit, the detection limit, and the determination limit. All of them were introduced in 1968 by Currie (1968), who standardised the terms that were used before him, and De Geer adapted in his 2004 work Currie's ideas specifically for gamma spectrometry.

The critical limit is used to concretely decide whether a signal is present or not: it is part of the process, in other words a posteriori limit.

$$L_C = k \cdot \sqrt{1.25 G B_C \omega_E \left(1+\frac{1}{m}\right)} \quad (1)$$

where k is the constant related to the assumed risk, G is the number of channels/kev, B_C is the measured background, ω_E is the FWHM given in keV and m is the number of times the background has been measured.

The detection limit is the limiting level that qualifies the procedure even before measurement; consequently, it's an a priori limit, and it tells us of how many of our detected counts are clearly detected: it provides the measurement a level of reliability.

$$L_D = k^2 + 2L_C \quad (2)$$

The determination limit, L_Q, above which the precision is considered well enough for quantitative determinations (De Geer, 2004). The former definitions of limiting levels were simply referring to the activity that can be determined with a given degree of confidence, so in other words, not making the difference between the a priori and a posteriori case.

$$L_Q = \gamma\sqrt{(2C_B)}\left\{k_\alpha\left[\sqrt{\left(1+\frac{k_\alpha^2}{8C_B}\right)}+\frac{k_\alpha}{\sqrt{8C_B}}\right]+k_\beta\left[1+\frac{k_\alpha^2}{4C_B}+\frac{k_\alpha}{\sqrt{2C_B}}\sqrt{\left(1+\frac{k_\alpha^2}{8C_B}\right)}\right]^{\frac{1}{2}}\right\} \quad (3)$$

$$L_Q \cong \gamma\left(k_\alpha + k_\beta\right)\sqrt{2C_B} \quad \text{when} \quad \frac{k_\alpha}{\sqrt{C_B}} \ll 1 \quad (4)$$

where γ - calibration constant, C_B - measured background count, k_α,k_β are constants.

In case of gamma peaks of which separation is not permitted by detector resolution, one important thing to

point out is the detection limits apply to an energy, and not to a specific transition (Șuvăilă, 2023). A very good example is the common 186 keV peak which comprises contributions from two different natural radionuclides with very close de-excitation energies, ^{226}Ra and ^{235}U: when we set detection limits, we do it for a certain region of interest (ROI), so the counts found in that specific area originate from both radionuclides. Their specific activity calculation needs to take into account weighing factors obtained by analysing peaks from the same species and the individual yields.

Currie limits revised (Currie, 1999) have been used by experts lately; it is now proven statistic testing of detection and decision limits is the only efficient way of getting close to their real values. This is the reason for which we calculate the decision limits solely this way and abandon any archaic expression of the latter.

2.5. Experimental measurements

In order to correctly estimate the detection limits, we proceeded first to the background and blank sample measurements, which were carried out with Rn purge and periodic stability tests, just as the measurements performed on the samples from the cores. After acquiring all the spectra which were needed, we irradiated a sample (of greater mass, for better statistics) in a thermal neutron flux of about 6×10^6 neutrons/second in 4π. Subsequently, that sample was re-measured, in order to evidence which other nuclei would be able to be evidenced in samples from this area. As a side note, all samples which are measured for their natural spectrum are entirely reusable, as opposite to those irradiated in a neutron flux, which activates the material and their containers: neutron activation analysis is meant to evidence nuclei that are present in the sample by measuring the resulting nuclei from the neutron reaction, as the initial ones would not emit any gammas, reason for which we irradiate them. Following the case, such a sample may be considered nuclear waste and treated as such, according to the recommendations of the Regulatory Commission for Nuclear Activities.

Spectra analysis was performed by using several software tools, particularly one under development by our group, named GaDeTool Geo (Gamma Decision Tool). This software is quite friendly, as it is capable of self-calibration in terms of energy, provided an environmental sample is measured. The automation level is very high; however, in any case of doubt, unusual shape of full energy peaks and so on, human decision is asked for in the end. After subtracting the areas from the blank samples (or the regions of interest – ROIs) from the unirradiated samples for those which underwent neutron flux interaction), we calculated the specific activities (SA - activities in Becquerels, or s^{-1}), for the radionuclides of interest, which are presented in the next section.

3. RESULTS AND DISCUSSION

In spite of the fact dry net mass of the sediment samples were very low, the results prove the measured quantities are above (or well above, following the case) the detection and decision limits, as shown in Table 1. The variability suggests isotopic patterns would be reliable in order to identify the spots from a batch and also allow tracking differences in the recent sedimentation processes by means of ^{210}Pb analysis.

However, the differences found in specific activities for same radionuclides in same samples following different energies analysed shows once again we need to renew the set of calibration sources in order to obtain the desired performance from our laboratory. The values are overall within the typical limits for environmental samples from this part of Europe. ^{137}Cs analysis shows the samples are clean radiologically speaking, but on the other hand we need to make efforts in order to lower detection limits again, as it is virtually impossible not to have traces of Caesium in a spot 600 km away from Chernobyl just 38 years after the tragic event. However, ^{137}Cs levels are not high in the area, and in the meantime this radioelement underwent diffusion in all layers, sometimes including upwards - in the layer which was added post-Cernobyl by sedimentation processes. Intercomparison between samples from the batch indicates natural radioelements concentrations are close enough to confirm the sampling area characteristics and still exhibit little differences, apparently specific to each core.

The Monte Carlo correction factor is the product of the auto attenuation coefficient, the real summing correction one, and the geometry transfer factor - the latter being equal to 1 here, as we prioritized geometry invariance for the setup.

Nuclear decay data is all taken from the Brookheaven National Laboratory (NNDC, 2023). Simulation data is all provided by GESPECOR (Sima *et al.*, 2001) updated to version 5.0 (2016).

Regarding the uncertainty budget, the greatest component was the one originating from the calibration sources, as they were old and need to be rapidly replaced. Once again, measurements relative to each other, or the ratios of the specific activities prove to be a very good indicator for isotopic pattern attribution.

A major improvement was made by optimising the electronic parameters, as we went from 1 kiloelectronvolt (keV) per channel in the MCA to 0.17 keV. The difference in resolution is shown in figure 6, a very benefic result of our optimisation work.

It is worth mentioning qualitative analysis after thermal neutron irradiation of the samples evidenced the presence of ^{56}Mn (at 847 and 2113 keV), ^{24}Na (1369 keV and 2755 keV) and ^{41}Ca (1812 keV) in different quantities, which opens the way to subsidiary oligoelement analysis.

Table 1. Experimental results from Lake Erenciuc

Element/keV	%	eff	MC corr	C2 10-13	SA 10-13	C2 18-21	SA 18-21	C2 26-29	SA 26-29	C2 34-37	SA 34-37	C2 42-44	SA 42-44	C1 45-47	SA 45-47	C3 51-54	SA 51-54
Pb-210 46.54	4.25	0.00057	1.0000	164.6	36.8	148.5	40.7	137.4	23.6	216.06	29.504	156.06	26.113	227.1	28.1	184.45	18.01
Th-234 63.29	3.72	0.00117	0.9999	3248.3	404.9	3097.0	472.9	2722.5	261.1	3505.5	266.95	3127.6	291.84	5554.8	383.5	3427.5	186.63
Th-234 92.59	4.25	0.00152	0.9998	4320.5	364.3	3704.4	382.6	3792.0	245.9	4912.8	253.06	4691.6	296.11	6269.7	292.8	4874.1	179.52
Ra-226 185.71*	3.56	0.00139	1.0000	1536.1	168.4	1178.0	158.2	1068.8	90.2	1578.1	105.71	1317.9	108.17	1915.1	116.3	1626.2	77.887
U/Ra tot	n/a	n/a	n/a	2694.9	176.4	2066.7	165.7	1875.1	94.4	2768.6	110.7	2312.1	113.3	3359.9	121.8	2852.9	81.6
U-235 185.71**	57.09	0.00139	0.9906	1158.8	7.9	888.7	7.4	806.3	4.2	1190.5	5.0	994.2	5.1	1444.8	5.5	1226.7	3.7
Pb-212 238.63	43.65	0.00122	0.9998	2761.6	28.2	2124.6	26.6	1722.2	13.5	3693.5	23.055	2565.7	19.624	4435.4	25.1	4337.3	19.358
Pb-214 295.24	18.41	0.00105	1.0010	1148.2	32.2	917.6	31.5	955.8	20.6	1744.2	29.851	1121.5	23.519	1857.9	28.8	2022.1	24.745
Ac-228 338.32	11.27	0.00095	0.9999	451.8	23.0	413.2	25.8	268.6	10.5	915.4	28.463	557.7	21.248	772.3	21.8	692.3	15.392
Pb-214 351.93	35.60	0.00092	0.9987	1958.7	32.6	1918.8	39.1	1836.5	23.5	3088.1	31.401	1745.3	21.745	3427.8	31.6	3086.4	22.44
Tl-208 583.19	85.00	0.00058	0.9998	1309.9	14.4	1407.2	19.0	1106.5	9.4	1548.8	10.402	1309.6	10.778	2008.7	12.2	1927.4	9.2563
Bi-214 609.31	45.44	0.00056	0.8799	3226.7	69.1	2751.7	72.2	2332.6	38.4	3033.6	39.674	2731.5	43.772	4249.5	50.4	3937.1	36.817
Ac-228 911.20	25.80	0.0004	0.8592	3990.6	209.4	3397.7	218.3	3108.6	125.4	4582.4	146.85	3357.5	131.84	5193.1	150.9	4686	107.38
Ac-228 968.97	15.80	0.00039	0.8601	2918.9	260.8	2189.4	239.6	2139.8	147.0	3187.3	173.93	2379	159.07	3640.0	180.1	3042	118.7
K-40 1460.75	10.66	0.0003	1.0000	6158.5	1045.4	5452.3	1133.6	5091.1	664.7	7202.1	746.8	5593.7	710.7	8374.1	787.2	6570.3	487.13
Tl-208 2614.53	99.75	0.00019	0.9879	1437.0	40.6	1276.6	44.1	1177.0	25.6	1632.4	28.155	1291.7	27.298	1927.0	30.1	1534.7	18.926
Cs-137 661.66	84.99	0.00052	1.0000	det/dec	det/dec	det/dec	det/dec	det/dec	det/dec	det/dec	det/dec	det/dec	det/dec	det/dec	det/dec	det/dec	det/dec
M(g)/LT*10^-3(s)	n/a	n/a	n/a	9.4/196	n/a	8.6/175	n/a	14.8/162	n/a	13.3/226	n/a	13.9/177	n/a	12.6/262	n/a	20.5/205	n/a

*57% of convoluted peak area; **43% of convoluted peak area; % is the decay yield

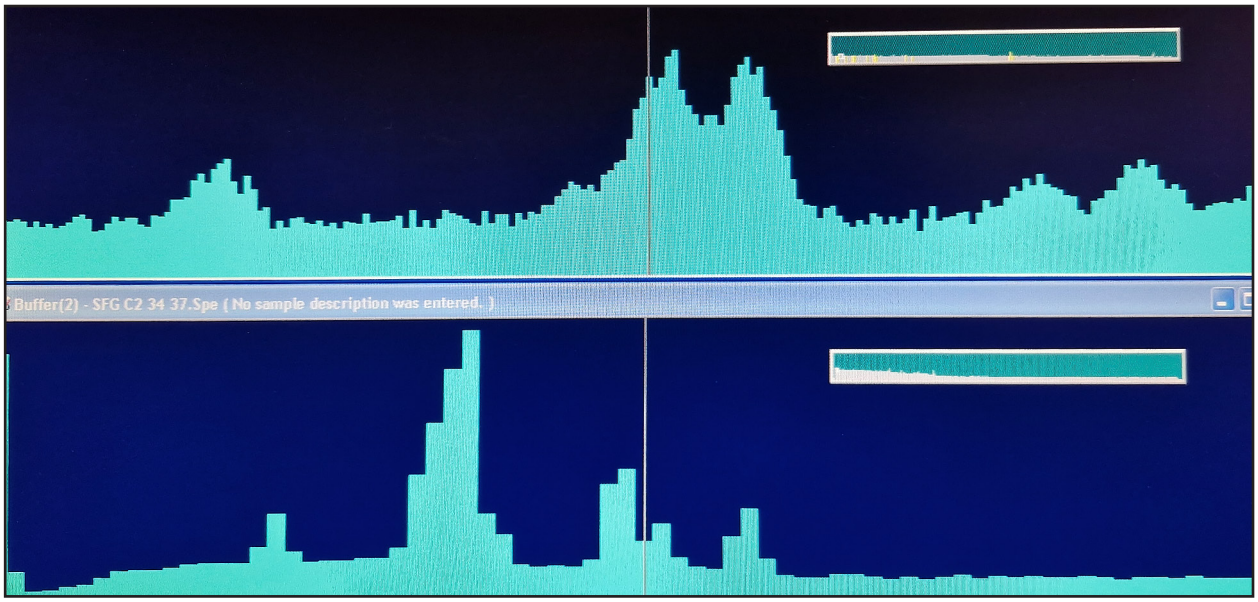

Fig. 6. Resolution change following electronics optimisation

4. CONCLUSIONS

The present work shows isotopic pattern can be studied and dating procedures can be applied successfully for samples originating from this area, provided the individual sample net mass exceeds some 20 g per layer of about 2 cm thickness in a reasonable spectrum acquisition time (about 24 h) with HPGe detectors of over 30% relative efficiency. Also, enhancing isotopic pattern recognition will be successful with thermal neutrons for irradiation times less than the spectrum acquisition time, provided the neutron flux is at least 5×10^3 in 4π.

The target standard combined uncertainty of 5% is achievable by combining two actions. The first is LN_2 purging the vicinity of the detector: Rn purge will allow lowering all its descendants activity by an order of magnitude, as it was shown by Șuvăilă *et al.* (2012). Also, adding an extra layer of lead shielding of another 5 cm and additional successive covering detector side surface with layers of Cadmium, Copper and Aluminum of 2 mm thickness each in order to cut the X rays would lower the background due to Pb characteristic X rays and low energy quanta resulting from the Compton interactions within the shield; this was simulated using the GESPECOR code.

The main need we currently have is to change the calibration sources with new, modern ones, more precise, tested for uniformity and reliability. In other terms, the new Gamma laboratory in GeoEcoMar is a success so far, a promising facility for extending our experimental capabilities for analysis of environmental radiation of nuclear origins both for the natural and anthropogenic cases.

ACKNOWLEDGEMENTS

The work was supported by the Ministry of Research, Innovation and Digitization (MCID), Core Programme 2023-2026 of INCD GeoEcoMar, Project PN 23 30 01 02.

REFERENCES

Currie, L.A. (1968). Limits for qualitative detection and quantitative determination. Application to radiochemistry. *Analytical Chemistry Journal* **40**: 586-593.

Currie, L.A. (1999). Detection and quantification limits: origins and historical overview. *Analytica Chimica Acta* **39** (*2*): 127-134.

De Geer, L.-E. (2004). Currie detection limits in gamma-ray spectroscopy. *Applied Radiation and Isotopes* **61**(*2-3*): 151-160.

Olăcel, A., Ujeniuc, S., Șuvăilă, R., Alexandrescu, B., Pojar, I. (2022). Isotopic patterns via neutron irradiation and gamma

spectrometry of environmental samples. *Chemical Physics Impact*, **4**: 1-4.

Sima, O., Arnold, D., Dovlete, C. (2001). GESPECOR: A versatile tool in gamma-ray spectrometry. *Journal of Radioanalytical and Nuclear Chemistry* **248**: 359-364.

Sima, O. (2022). Faculty of Physics, University of Bucharest, *private communication*.

Șuvăilă, R., Sima, O. (2011). Complex Gamma Ray Spectra Analysis. *Romanian Reports in Physics*, **63**(*4*): 975-987.

Șuvăilă, R. (2023). Faculty of Physics, University of Bucharest, *interdisciplinary gamma spectroscopy course*.

Șuvăilă, R., Sima, O., Vîrgolici, M., Ponta, C.C., Cutrubinis, M., Teodor, E.S., Nicolae C.M. (2012). Gamma ray spectroscopy for artificial contamination effects evaluation in luminiscence dating of artefacts from low depth layers in southern Romania, *Romanian Reports in Physics*, **64** (*2*): 381-386.

https://nndc.bnl.gov